Proceedings of the 21st ICSMGE, Vienna, Austria, 14 – 19 June 2026. Pistrol, Adam & Schweiger (eds.)
Published by: ÖGG, Austrian Society for Geomechanics, Salzburg, Austria, ISBN 978-3-9503898-4-5
https://doi.org/10.53243/ICSMGE2026-374

A Real-Time Decision-Making Framework for Post-Flood Road Closure in Moisture-Sensitive Unbound Granular Pavements

Ayesh Dushmantha, Chaminda Gallage
School of Civil and Environmental Engineering, QUT, Brisbane, Australia, ayesh.gamaralalage@hdr.qut.edu.au

Jinjiang Zhong
Logan City Council, Logan, Queensland, Australia

ABSTRACT: Unbound Granular Materials (UGMs) are a cost-effective and widely used component of road pavements in Australia, particularly in low-traffic regions. However, their performance is highly sensitive to moisture ingress resulting from rainfall and flooding, especially in areas exposed to extreme climatic conditions. This study investigates the critical thresholds at which UGMs begin to lose structural integrity as saturation increases. Repeated Load Triaxial (RLT) tests were conducted to evaluate two key performance indicators, resilient modulus (M_r) and plastic strain (ε_p), under varying Degrees of Saturation (DoS) and stress levels. The results reveal that M_r increases with DoS up to a critical threshold (DoS = 0.83), beyond which it declines sharply. Simultaneously, ε_p exhibits exponential growth under high saturation. These trends were modelled using newly developed empirical equations, enabling the identification of a "DoS range of vulnerability to damage". The developed models achieved high accuracy (R^2 = 0.98 for M_r and R^2 = 0.86 for ε_p) and were validated using literature-based data (R^2 > 0.95 for both M_r and ε_p). By integrating these models with real-time sensor data, critical periods of moisture exceedance were identified under both normal and extreme climatic conditions. This facilitates improved real-time pavement management during critical situations such as flooding, as guided by the proposed procedure.

KEYWORDS: Unbound Granular Pavements, Moisture Dependent Resilient Modulus, Flood, Road resilience, Real time pavement Monitoring

1 INTRODUCTION

Australia's extensive road network spans over 900,000 km and is vital for maintaining connectivity, particularly in rural and regional areas (Clark & Gallage, 2020, Clark et al., 2018, Klompmaker et al., 2024, Gedara & Udukumburage, 2024, Cheah et al., 2016). A large portion of this network comprises low-volume roads, commonly constructed using UGMs due to their affordability, availability, and satisfactory performance under standard traffic loads (Jayalath et al., 2024, Dushmantha et al., 2024, Jayalath et al., 2021, Austroads, 2017, Weerasinghe et al., 2019). These materials, such as gravel, crushed rock, and lateritic soils, derive strength from interparticle friction and matric suction when unsaturated (Dutta & Kodikara, 2022, Sangsefidi et al., 2021). However, their performance deteriorates significantly under saturated conditions, leading to a loss of suction-induced cohesion and mechanical stability (Jayakody Arachchige et al., 2012, Gallage et al., 2012, Gallage et al., 2013a, Gallage et al., 2017, Gui et al., 2022).

Given Australia's climatic diversity, from arid zones to tropical regions, UGMs are particularly vulnerable to moisture variation, which is exacerbated by projected increases in extreme rainfall due to climate change. For instance, the 2022 Queensland floods caused over AUD 500 million in road damage (Deloitte Access Economics, 2022), and rainfall intensity is projected to increase by 15–30% by 2050 (Takhellambam et al., 2024, Wang et al., 2014). Understanding how moisture affects UGM behaviour under repeated traffic loading is therefore essential to ensuring long-term pavement resilience.

Two key parameters commonly used to evaluate UGM performance are the resilient modulus (M_r) and accumulated plastic strain (ε_p). M_r quantifies elastic recovery under cyclic loading and is a cornerstone of mechanistic-empirical design (Dushmantha et al., 2025a, Li et al., 2019, Chowdhury et al., 2021), while ε_p captures irreversible deformation linked to rutting (Gu et al., 2016, Gu et al., 2017, Luan et al., 2023, Dareeju et al., 2017, Jayakody et al., 2019, Ishikawa et al., 2021). Excessive ε_p can accelerate surface degradation by promoting water ponding and undermining structural capacity (Dushmantha et al., 2025b, Dushmantha & Gallage, 2025, Dutta et al., 2024, Xiao et al., 2018, Askarinejad et al., 2018, Cheah et al., 2017).

Among all influencing factors, moisture content is particularly dynamic and externally driven, governed by climatic elements such as rainfall, temperature, humidity, wind, and solar radiation (Maha Madakalapuge et al., 2022, Maha Madakalapuge et al., 2024, Dushmantha & Jayakody). Increases in moisture, especially beyond optimum compaction levels, reduce suction (Udukumburage et al., 2019, Abeykoon et al., 2017, Abeykoon et al., 2018) and interparticle resistance, leading to lower M_r and higher ε_p (Rahman & Erlingsson, 2016a, Rahman & Erlingsson, 2016b, Kodikara et al., 2014). Laboratory evidence confirms that a rising DoS correlates with reduced stiffness and increased deformation (Dutta & Kodikara, 2022, Gallage et al., 2013b), and these effects are amplified under traffic-induced cyclic loading (Alnedawi et al., 2018, Gallage et al., 2015).

Despite substantial experimental research, two critical knowledge gaps remain. First, there is no consensus on the critical DoS threshold at which UGMs shift from stable to degrading behaviour. For example, Dutta & Kodikara (2022) reported a peak M_r at DoS = 0.4 using a Constant Radial Stiffness Test (CRST), whereas Tatsuoka & Correia (2018) noted performance degradation at DoS = 0.7 based on CBR tests. Other studies using Geogauge data (Pu, 2002) and further laboratory trials (Dutta et al., 2024) showed considerable variability, with stiffness loss occurring below the optimum DoS. These inconsistencies likely stem from material differences, test setups, and moisture regimes, making it difficult to generalise findings for design applications.

Second, real-time moisture monitoring remains underutilised in current asset management practices. While embedded sensors have proven effective in capturing in-situ moisture dynamics (Ahmed et al., 2018, Hedayati & Hossain, 2015), their integration into predictive or preventive maintenance frameworks is limited. As a result, most agencies rely on reactive strategies, which can incur up to 60% higher lifecycle costs compared to timely, moisture-informed interventions (Mia et al., 2015).

This study addresses these gaps through a combined laboratory–field methodology, linking RLT test results with continuous field monitoring of DoS using embedded sensors. The goal is to identify the critical DoS threshold where UGM behaviour transitions from favorable to unfavourable, and to define the associated vulnerability window in field conditions. Empirical models will be developed to relate M_r and ε_p to DoS and Stress Ratio (SR), tailored to local materials, and validated against external datasets to ensure transferability.

Beyond technical advancements, this work supports broader resilience goals, aligning with UN Sustainable Development Goal 9 on resilient infrastructure (Brodny & Tutak, 2023, Monaco, 2024). By identifying moisture-related risk periods, the models aid targeted interventions such as drainage upgrades and optimised maintenance, while also informing climate-adaptive pavement design using real-time and projected moisture data.

2 METHODOLOGY

2.1 *Real-time moisture monitoring and materials*

To monitor temporal moisture variations within pavement layers, nine sensors were installed, three each in the base (100 mm), subbase (200 mm), and subgrade (400 mm), to capture vertical moisture gradients (Figure 1). These sensors were connected to cellular-enabled dataloggers for hourly data collection and were calibrated in-house for each pavement materials.

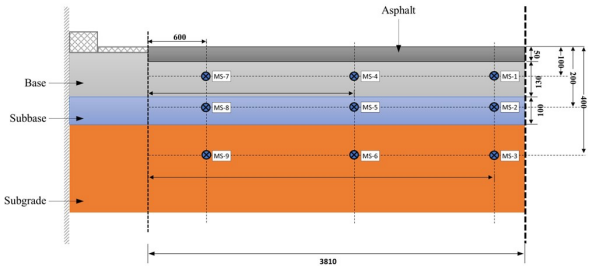

Figure 1. Sensors Installation Plan.

Among the three monitored layers, the base exhibited the greatest moisture variability, with DoS ranging from 0.56 to 1.00, due to its direct exposure to climatic influences. This layer was therefore selected for detailed laboratory characterisation. Material samples retrieved during sensor installation were tested following relevant Australian Standards, including particle size distribution (AS 1289.3.6.1), liquid limit (AS 1289.3.9.1 – 2009), plasticity index (AS 1289.3.9.1 – 2015), and specific gravity (AS 1289.3.5.1 – 2006). Maximum Dry Density (MDD) and Optimum Moisture Content (OMC) were assessed under three regimes: reduced effort (357 kJ/m³), standard Proctor (569 kJ/m³; AS 1289.5.1.1 – 2007), and modified Proctor (2,677.5 kJ/m³; AS 1289.5.2.1 – 2017). The Line of Optimum (LOO), representing the DoS at peak dry density, was found to be 0.90. According to the Unified Soil Classification System (USCS), the material was classified as well-graded gravel with significant sand content (GW). Key geotechnical properties are listed in Table 1.

Table 1. Basic Soil parameters

Parameter	Value
D10 (mm)	0.42
D50 (mm)	3.10
D60 (mm)	4.80
Liquid Limit (LL) (%)	22
Plasticity Index (PI)	NP
Specific Gravity ($\mathbf{G_s}$)	2.77
Reduced Proctor – OMC (%)	8.6
Reduced Proctor – MDD (g/cm³)	2.19
Standard Proctor – OMC (%)	6.4
Standard Proctor – MDD (g/cm³)	2.32
Modified Proctor – OMC (%)	4.7
Modified Proctor – MDD (g/cm³)	2.42
Average Field Dry Density (g/cm³)	2.31

2.2 *Repeated Load Triaxial testing*

To evaluate the mechanical response of UGMs under cyclic loading and varying moisture conditions, RLT tests were conducted. This method assesses two key performance indicators, M_r, reflecting elastic stiffness, and permanent strain (ε_p), representing cumulative deformation. A schematic of the typical stress–strain response observed during testing is shown in Figure 2.

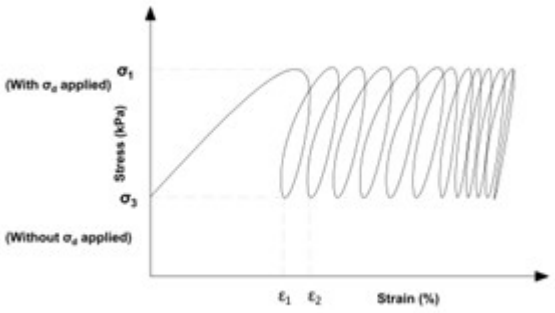

Figure 2. Typical stress-strain diagram during RLT test.

The M_r was computed as the ratio of deviator stress ($\sigma_d = \sigma_1 - \sigma_3$) to the recoverable axial strain (ε_r), while permanent strain (ε_p) was determined from the incremental change in axial strain between load cycles. Specimens (100 mm × 200 mm) were compacted to the MDD derived from the standard Proctor test and subjected to deviator stresses of 250, 375, 500, and 625 kPa, yielding stress ratios ($SR = \frac{\sigma_d}{\sigma_3}$) from 2 to 5. Moisture conditions were controlled at DoS levels of 0.65, 0.75, 0.85, and 0.95, reflecting observed in-field moisture variations. Sixteen tests were performed following standard Q137 and, to ensure repeatability, three replicates were conducted under a representative test case, confirming the consistency and reliability of results.

3 RESULTS AND DISCUSSION

3.1 *Initial Observation of Moisture Dynamics from Real-Time Measured Data*

A long-term field monitoring program was carried out from September 2020 to July 2023 at a pavement site in Queensland, Australia, to investigate moisture behaviour across pavement layers. Three moisture sensors were embedded in each layer, with averaged readings used to generate representative DoS trends. The resulting time series enabled evaluation of both long-term moisture variation and short-term responses to flood events. Figure 3 and Figure 4 illustrate DoS changes over two half-year periods and during a selected flood event, respectively.

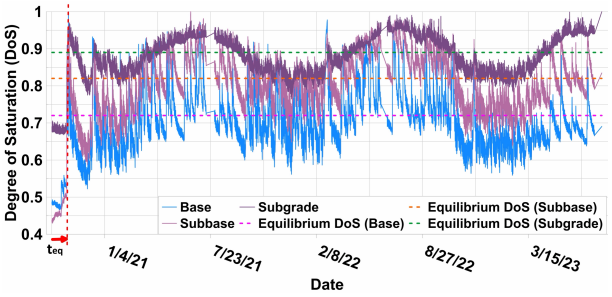

Figure 3. DoS variation of pavement layers.

Key moisture-related parameters were extracted, including the equilibrium DoS (DoS_{eq}), variation range, and environmental sensitivity across pavement layers. The base layer, closest to the surface, showed the lowest DoS_{eq} (0.72) and highest variability (0.56–1.00), reflecting strong responsiveness to surface climate conditions. The subbase exhibited moderate values (DoS_{eq} = 0.82; range = 0.63–1.00), while the subgrade showed the highest DoS_{eq} (0.89) with minimal variation (0.77–1.00), likely less influenced by land climate interactions. These results confirm a clear depth-dependent attenuation of moisture dynamics, underscoring the importance of layer-specific analysis.

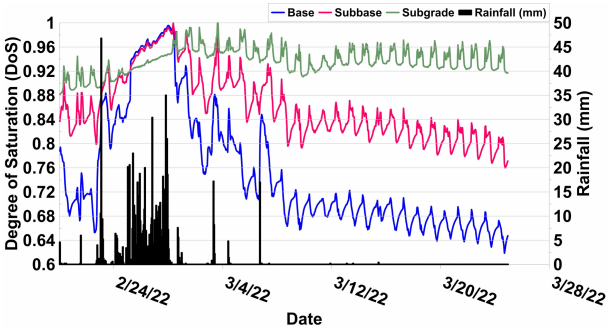

Figure 4. DoS variation during a flood event

Initial post-installation data indicated that the pavement system required approximately 24 days to reach moisture equilibrium following sensor embedding, as shown in Figure 3. This period, characterised by repeated wetting and drying cycles, reflects the natural adjustment process of pavement layers under climatic exposure and moisture redistribution (Dushmantha & Gallage, 2025, Madakalapuge et al., 2022).

During the extreme flood event illustrated in Figure 4 the base layer demonstrated the fastest drop in DoS post-rainfall, confirming its high drainage capacity and exposure to drying. In contrast, the subbase exhibited slower moisture loss, while the subgrade remained nearly saturated for nearly four weeks, likely due to low permeability and proximity to the water table. These findings confirm that the base layer is the most responsive to moisture changes and structurally critical, justifying its selection for RLT testing. This allowed a detailed investigation into its resilient and plastic performance under varying DoS, directly linked to field-monitored moisture conditions.

3.2 *Repeated Load Triaxial (RLT) test*

The mechanical behaviour of the base layer under varying stress and moisture conditions was assessed using an extensive RLT testing program. The evaluation focused on two key parameters, M_r and ε_p across a range of DoS values. Two key behavioral trends have emerged. Firstly, M_r consistently increased with rising SR across all moisture levels, reflecting stress-induced stiffness gain typical of granular materials. However, when stress was held constant, M_r displayed a non-linear trend, initially increasing with DoS before dropping sharply near full saturation, due to the loss of matric suction and particle interlock that maintain stiffness in unsaturated conditions.

Secondly, ε_p was influenced by both SR and DoS, but moisture had the dominant effect. While ε_p rose modestly with SR at fixed saturation, it increased exponentially with the rising DoS under constant stress. This trend highlights the role of moisture in promoting shear deformation and particle rearrangement in unbound materials. Together, these findings underscore the critical vulnerability of UGMs at high saturation, where reduced stiffness and rapid deformation co-occur.

3.2.1 *Resilient Modulus (M_r)*

From the RLT tests, Figure 5 illustrates the resilient response of the tested UGM under combined variations in SR and DoS. The results reveal a nonlinear response, highlighting the complex interaction between mechanical loading and moisture conditions.

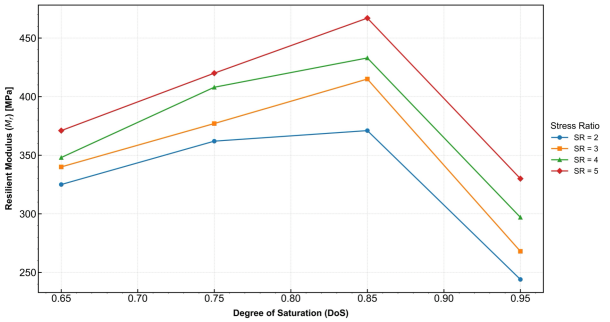

Figure 5. Variation of Resilient Modulus with SR and DoS.

The interaction between SR and moisture conditions significantly influences the M_r of UGMs. Three distinct behavioral trends were observed in the experimental results. First, under constant moisture content, M_r increased with SR, reflecting stress-induced stiffening due to enhanced bulk stress and internal particle rearrangement. For example, at DoS = 0.85, M_r rose from 371 MPa (SR = 2) to 467 MPa (SR = 5), an increase of approximately 26 %, consistent with known densification mechanisms in granular materials.

Second, when stress was held constant, M_r declined with increasing DoS, particularly beyond the critical threshold (DoS > 0.83), where matric suction and interparticle friction diminish. At SR = 4, M_r dropped from 433 MPa at DoS = 0.85 to 297 MPa at DoS = 0.95, a 31% reduction, demonstrating moisture-induced softening, as similarly reported by Rahman and Erlingsson (2015). Third, at near-saturation (DoS = 0.95), all specimens showed early failure, indicating reduced effective stress and potential onset of liquefaction. This underscores the instability of UGMs under extreme moisture conditions. To quantify these interactions, a predictive model was developed for M_r as a function of SR and DoS (Equation (1) and Equation (2))

$$M_r = A\,(1+SR)^B.f\,(DoS) \quad (1)$$

$$f(DoS) = p + q\,DoS + r\,DoS^2 + s\,DoS^3 + t\,DoS^4 \quad (2)$$

Where, A, B, p, q, r, s and t are model parameters and f is a function that depends on the DoS. The proposed model demonstrated excellent performance, achieving a high level of accuracy with an R^2 value of 0.98 when fitted to the test results. The determined parameters for the model are as follows: A =

45.4213, B = 0.2801, p = 69.5867, q = -197.4417, r = 63.5522, s = 262.0396, and t = -196.2986, specifically for the tested UGM.

This model was validated using existing data from Sun et al. (2021), achieving a high accuracy with an R^2 value of 0.98, demonstrating its robustness across different materials.

3.2.2 *Plastic Strain (ε_p)*

Accumulated plastic strain (ε_p) is the second critical indicator of long-term deformation in UGMs, capturing permanent changes under cyclic loading, unlike the resilient modulus, which reflects elastic recovery. Results from the RLT testing program demonstrated that ε_p is strongly influenced by both SR and DoS. As illustrated in

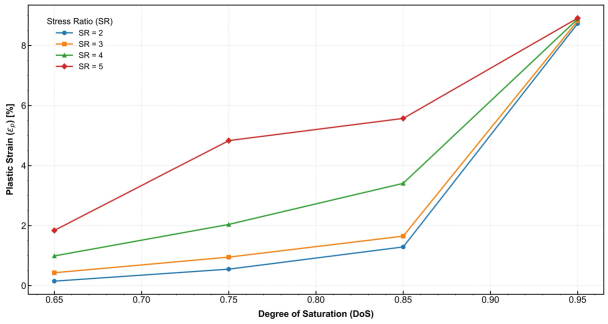

Figure 6, ε_p consistently increased with rising SR and DoS, confirming a coupled hydro-mechanical interaction driving progressive deformation in pavement layers.

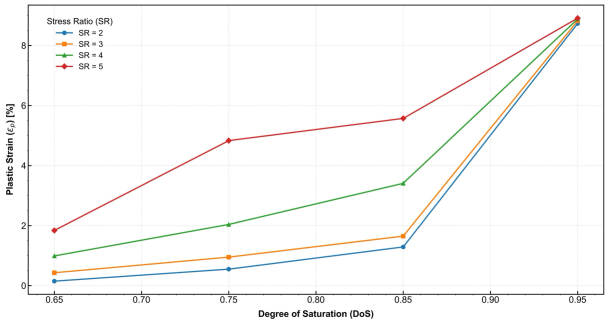

Figure 6. Variation of Plastic Strain with SR and DoS.

At lower SRs (≤ 3), the tested UGM exhibited signs of strain stabilisation, indicating a transition into a shakedown state, where further cyclic loading resulted in minimal additional plastic deformation. For instance, at DoS = 0.75 and SR = 2, ε_p plateaued at 0.55 %, suggesting that internal particle rearrangement had achieved mechanical equilibrium. A similar trend was observed at SR = 3, where ε_p stabilised at 0.95 % (DoS = 0.75) and 1.65 % (DoS = 0.85).

In contrast, under higher SRs (≥ 4), the material displayed progressive accumulation of ε_p throughout the entire loading sequence, with no indication of stabilisation. At SR = 4 and DoS = 0.85, ε_p reached 3.41%, increasing to 5.57% at SR = 5 under the same saturation. This rapid increase reflects the transition to a progressive failure regime, primarily driven by elevated moisture, which reduces interparticle friction and suction, facilitating enhanced deformation.

At near-saturation (DoS = 0.95), the deformation response became predominantly governed by moisture, with ε_p peaking at 8.91% (SR = 5). Notably, under this condition, the influence of SR diminished, and high strain levels were observed consistently across all stress levels. This behaviour suggests a shift toward a lubrication-controlled regime, where excess pore water enables unrestricted particle movement and shear-induced displacement, consistent with findings by Ma et al. (2020). To capture these trends quantitatively, an empirical model was developed to express ε_p as a function of SR and DoS (Equation (3) and Equation (4)).

$$\varepsilon_p = C\,(1+SR)^D . f\,(DoS) \quad (3)$$

$$f(DoS) = e^{E*DoS} \quad (4)$$

Where, C, D, and E, are model parameters and f is a function that depends on the DoS. The proposed model demonstrated strong performance, achieving a high level of accuracy with an R^2 value of 0.86 when fitted to the test results. The determined parameters for the model are as follows: C = 0.0022, D = 0.3112, and E = 8.3203, specifically for the tested UGM. Furthermore, the model was validated using data from Sun et al. (2021), achieving an R^2 value of 0.96, confirming its reliability across different datasets.

3.3 *Integration of Field DoS Variation and RLT Test Results*

A major contribution of this study lies in linking laboratory-derived strength parameters, M_r and ε_p, with real-time field moisture data, quantified as DoS (Figure 7). This integration allows for the identification of critical time windows during which the pavement base layer is most vulnerable to structural degradation. These periods typically coincide with elevated moisture levels and active loading, resulting in reduced stiffness and greater permanent deformation. To align with field conditions, a SR of 6 was adopted, corresponding to a vertical tyre pressure of 750 kPa and a confining pressure of 125 kPa.

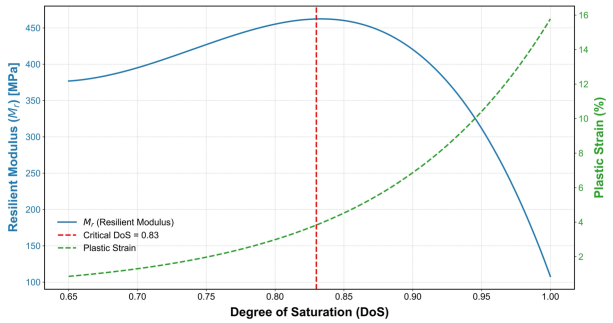

Figure 7. Variation of Resilient Parameters with DoS

Under these conditions, M_r peaked at DoS = 0.83, beyond which a sharp decline was observed, indicating a critical moisture threshold associated with accelerated stiffness loss. In parallel, ε_p increased significantly beyond this point, reflecting reduced interparticle resistance and growing deformation potential. This critical threshold was subsequently applied to field-measured DoS data to identify periods of exceedance and associated pavement vulnerability (Figure 8 and Figure 9)

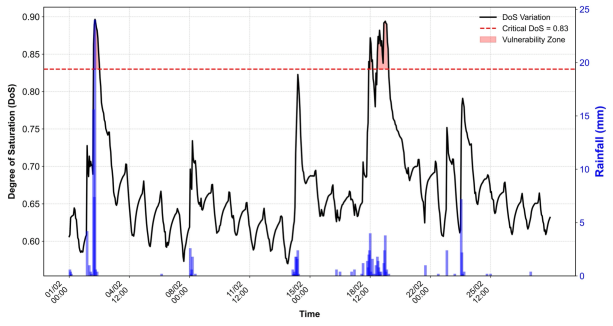

Figure 8. Vulnerability window for February 2021.

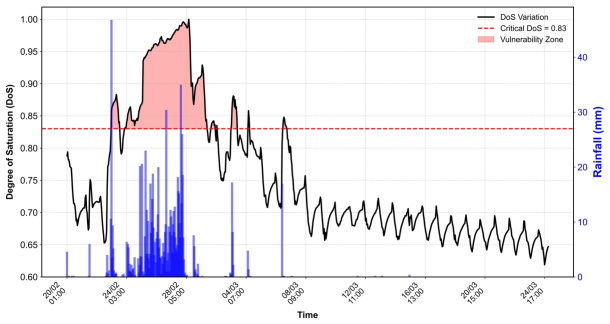

Figure 9. Vulnerability window for February 2022.

Analysis of field data revealed distinct differences in pavement moisture exposure under normal and extreme conditions. During a typical seasonal month (February 2021), the DoS exceeded the critical threshold (0.83) for only 30 hours out of 672 (≈ 4.5 %), with short, isolated events suggesting minimal risk under standard traffic loads. However, in February 2022, during a major flood, the DoS remained above the threshold for 176 hours, representing over 22 % of the 791-hour period. This prolonged saturation period indicated compromised structural conditions. Extended exposure to high DoS increases the risk of rutting, deformation, and early failure, particularly in the base layer. These findings highlight the value of coupling laboratory-defined moisture-performance thresholds with real-time field data to enable moisture-responsive pavement assessment.

4 CONCLUSIONS

This study introduced an integrated methodology for assessing pavement performance by combining two years of real-time moisture data with laboratory-based strength parameters derived from Repeated Load Triaxial (RLT) testing. The focus was on the base layer constructed with unbound granular material (UGM), which exhibited the highest moisture variability (DoS range: 0.56 – 1.00) due to its proximity to the surface. In contrast, the subbase and subgrade showed progressively narrower variation ranges and higher equilibrium saturation values, confirming reduced moisture sensitivity with depth.

RLT results demonstrated that the M_r increased with both stress ratio and DoS up to a critical saturation point (DoS = 0.83), beyond which it declined sharply due to moisture-induced softening. Plastic strain (ε_p) increased exponentially with saturation, especially under higher stress levels, indicating a transition toward permanent deformation at elevated moisture states. Two predictive models were developed to describe M_r and ε_p as functions of stress and saturation. These models showed high accuracy ($R^2 = 0.98$ for M_r, $R^2 = 0.86$ for ε_p) and were successfully validated using literature data, confirming their reliability and applicability for pavement performance evaluation.

By applying the critical DoS threshold to field-monitored data, the study identified moisture-exceedance periods linked to pavement vulnerability. A typical dry month (Feb 2021) showed limited exceedance (30 hours or 4.5% of the time), whereas the 2022 flood event resulted in prolonged saturation (176 hours or 22%), revealing extended structural exposure to damaging conditions.

These findings underscore the value of integrating mechanical response models with real-time hydrological data to support moisture-responsive pavement management. The proposed framework enables timely identification of risk periods and facilitates adaptive maintenance planning, particularly for climate-exposed and flood-prone road networks.

5 ACKNOWLEDGEMENTS

The authors gratefully acknowledge the financial and intellectual support provided by the Queensland University of Technology (QUT) through its Higher Degree Research (HDR) program. In particular, the scholarship awarded to the first author was instrumental in facilitating the successful completion of this research. The authors also express their sincere appreciation to Logan City Council (LCC) for granting access to the trial site used for sensor installation and long-term data collection, which formed a critical component of this study.

6 REFERENCES

Abeykoon, A., Gallage, C., Dareeju, B. & Trofimovs, J. 2018. Real-time monitoring and wireless data transmission to predict rain-induced landslides in critical slopes. *Australian Geomechanics Journal,* 53**,** 61-76.

Abeykoon, A., Udukumburage, R. S., Gallage, C. & Uchimura, T. 2017. Comparison of direct and indirect measured soil-water characteristic curves for a silty sand. *International Journal of GEOMATE,* 13**,** 9-16.

Ahmed, A., Hossain, S., Khan, M. S. & Shishani, A. 2018. Data-Based Real-Time Moisture Modeling in Unsaturated Expansive Subgrade in Texas. *Transportation Research Record: Journal of the Transportation Research Board,* 2672**,** 86-95.

Alnedawi, A., Nepal, K. P. & Al-Ameri, R. 2018. Permanent Deformation Prediction Model of Unbound Granular Materials for Flexible Pavement Design. *Transportation Infrastructure Geotechnology,* 6**,** 39-55.

Askarinejad, H., Barati, P., Dhanasekar, M. & Gallage, C. 2018. Field studies on sleeper deflection and ballast pressure in heavy haul track. *Australian journal of structural engineering,* 19**,** 96-104.

Austroads 2017. Guide to Pavement Technology Part 2 Pavement Structural Design. Sydney, Australia.: Austroads Ltd., Level 9, 287 Elizabeth Street, Sydney NSW 2000, Australia.

Brodny, J. & Tutak, M. 2023. Assessing regional implementation of Sustainable Development Goal 9 "Build resilient infrastructure, promote sustainable industrialization and foster innovation" in Poland. *Technological Forecasting and Social Change,* 195**,** 122773.

Cheah, C., Gallage, C., Dawes, L. & Kendall, P. 2016. Impact resistance and evaluation of retained strength on geotextiles. *Geotextiles and Geomembranes,* 44**,** 549-556.

Cheah, C., Gallage, C., Dawes, L. & Kendall, P. 2017. Measuring hydraulic properties of geotextiles after installation damage. *Geotextiles and Geomembranes,* 45**,** 462-470.

Chowdhury, S. M. R. M., Kassem, E., Alkuime, H., Mishra, D. & Bayomy, F. M. S. 2021. Summary Resilient Modulus Prediction Model for Unbound Coarse Materials. *Journal of Transportation Engineering, Part B: Pavements,* 147.

Clark, B. R. & Gallage, C. 2020. Superior performance benefits of multigrade bitumen asphalt with recycled asphalt pavement additive. *Construction and Building Materials,* 230**,** 116963.

Clark, B. R., Piacere, L. & Gallage, C. 2018. Effects of recycled asphalt pavement on the stiffness and fatigue performance of multigrade bitumen asphalt. *Journal of Materials in Civil Engineering,* 30**,** 04017278.

Dareeju, B., Gallage, C., Ishikawa, T. & Dhanasekar, M. 2017. Effects of principal stress axis rotation on cyclic deformation characteristics of rail track subgrade materials. *Soils and Foundations,* 57**,** 423-438.

Deloitte Access Economics 2022. The cost of South East Queensland's 2022 rainfall and flooding event. Brisbane, Australia: Queensland Reconstruction Authority.

Dushmantha, A. & Gallage, C. 2025. Numerical Approach to Moisture Prediction in Thin Sealed Pavements under Rainfall Influence. *Results in Engineering***,** 106079.

Dushmantha, A. & Jayakody, S. PREDICTIVE MODELLING OF MOISTURE DYNAMICS IN UNBOUND GRANULAR

PAVEMENTS USING REAL-TIME SENSOR DATA AND PRECIPITATION. The 15th International Conference on Sustainable Built Environment (ICSBE) 2024. 1479.

Dushmantha, A., Jayakody, S., Gui, Y. & Gallage, C. 2025a. A comprehensive review of the resilient behaviour of unbound granular pavement materials. *Journal of Traffic and Transportation Engineering (English Edition)*.

Dushmantha, A., Jayakody, S., Gui, Y., Zhong, J., Southon, A., FitzChance, Z. & Gallage, C. Towards Safer Roads Post-flooding: Moisture-Induced Pavement Behaviour and Recovery Times. International Conference on Transportation Geotechnics, 2024. Springer, 269-277.

Dushmantha, A., Zhang, R., Gui, Y., Zhong, J. & Gallage, C. 2025b. Deploying machine learning for long-term road pavement moisture prediction: A case study from Queensland, Australia. *Journal of Road Engineering,* 5**,** 184-201.

Dutta, T. T. & Kodikara, J. 2022. Evaluation of unbound/subgrade material rutting and resilient behaviour based on initial density and saturation degree. *Transportation Geotechnics,* 35.

Dutta, T. T., Tophel, A. & Kodikara, J. 2024. Resilient and rutting response of unbound granular material and subgrade soil influenced by initial state and stress conditions. *Road Materials and Pavement Design***,** 1-33.

Gallage, C., Cochrane, M. & Ramanujam, J. 2012. Effects of lime content and amelioration period in double lime application on the strength of lime treated expansive sub-grade soils. *Electrical Measuring Instruments and Measurements***,** 21.

Gallage, C., Dareeju, B. S. S. S. & Dhanasekar, M. State-of-the-art: track degradation at bridge transitions. Proceedings of the 4th international conference on structural engineering and construction management 2013, 2013a. Nethwin Printers (Pvt) Ltd, 40-52.

Gallage, C., Eom, T., Barker, D. & Ramanujam, J. Falling Weight Deflectometer (FWD) tests on granular pavement reinforced with geogrids-Case study. Geotechnics for Sustainable Development: Proceedings of the 2015 International Conference on Geotechnical Engineering (ICGE), 2015. Sri Lankan Geotechnical Society (SLGS), 597-600.

Gallage, C., Kodikara, J. & Uchimura, T. 2013b. Laboratory measurement of hydraulic conductivity functions of two unsaturated sandy soils during drying and wetting processes. *Soils and Foundations,* 53**,** 417-430.

Gallage, C., Tehrani, N. & Williams, D. Instrumented large soil-column to investigate climate-induced ground deformation in expansive soil. Proceedings of the 19th international conference on soil mechanics and geotechnical engineering, 2017. International Society for Soil Mechanics and Geotechnical Engineering, 1147-1150.

Gedara, G. & Udukumburage, S. 2024. VALIDATION OF SWELLING ESTIMATION METHODS USING A LABORATORY-SCALED INSTRUMENTED SOIL COLUMN. *GEOMATE Journal,* 27**,** 112-119.

Gu, F., Zhang, Y., Droddy, C. V., Luo, R. & Lytton, R. L. 2016. Development of a New Mechanistic Empirical Rutting Model for Unbound Granular Material. *Journal of Materials in Civil Engineering,* 28.

Gu, F., Zhang, Y., Luo, X., Sahin, H. & Lytton, R. L. 2017. Characterization and prediction of permanent deformation properties of unbound granular materials for pavement ME design. *Construction and Building Materials,* 155**,** 584-592.

Gui, Y., Wong, W. Y. & Gallage, C. 2022. Effectiveness and sensitivity of fiber inclusion on desiccation cracking behavior of reinforced clayey soil. *International Journal of Geomechanics,* 22**,** 06021040.

Hedayati, M. & Hossain, S. 2015. Data based model to estimate subgrade moisture variation case study: Low volume pavement in North Texas. *Transportation Geotechnics,* 3**,** 48-57.

Ishikawa, T., Dareeju, B., Gallage, C. & Tianshu, L. 2021. Resilient Deformation Characteristics of Unsaturated Subgrade Materials of Rail Tracks under Cyclic Moving Wheel Loads. *Geotechnical Engineering (00465828),* 52.

Jayakody Arachchige, S. P., Gallage, C. & Kumar, A. Assessment of recycled concrete aggregates for road base and sub-base. Proceedings of the second international conference on geotechnique, construction materials and environment, 2012. The GEOMATE International Society, 575-579.

Jayakody, S., Gallage, C. & Ramanujam, J. 2019. Performance characteristics of recycled concrete aggregate as an unbound pavement material. *Heliyon,* 5.

Jayalath, C., Gallage, C. & Wimalasena, K. 2024. Performance Characteristics of Black Vertosol as a Subgrade Material in Unpaved Granular Pavements. *International Journal of Pavement Research and Technology,* 17**,** 240-257.

Jayalath, C., Gallage, C., Wimalasena, K., Lee, J. & Ramanujam, J. 2021. Performance of composite geogrid reinforced unpaved pavements under cyclic loading. *Construction and Building Materials,* 304**,** 124570.

Klompmaker, J., Shahkolahi, A. & Gallage, C. 2024. Feldversuche zu Geogitter stabilisierten Tragschichten mit gebundenem Oberbau über weichem Untergrund mit hohem Quellvermögen. *geotechnik,* 47**,** 296-301.

Kodikara, J., Rajeev, P., Chan, D. & Gallage, C. 2014. Soil moisture monitoring at the field scale using neutron probe. *Canadian Geotechnical Journal,* 51**,** 332-345.

Li, N., Wang, H., Ma, B. & Li, R. 2019. Investigation of unbound granular material behavior using precision unbound material analyzer and repeated load triaxial test. *Transportation Geotechnics,* 18**,** 1-9.

Luan, Y., Ma, Y., Ma, T. & Xia, F. 2023. Investigation on the effects of physical property and stress state of graded crushed stone on resilient modulus and permanent deformation. *Construction and Building Materials,* 400.

Madakalapuge, C. M., Dutta, T. T., Bodin, D. & Kodikara, J. 2022. Numerical evaluation of temporal moisture variations in unbound pavements with thin seals. *Transportation Geotechnics***,** 100787.

Maha Madakalapuge, C., Dutta, T. T., Bodin, D. & Kodikara, J. 2022. Numerical evaluation of temporal moisture variations in unbound pavements with thin seals. *Transportation Geotechnics,* 35.

Maha Madakalapuge, C., Dutta, T. T. & Kodikara, J. 2024. Evaluation of climatic effects on moisture variation and performance of unbound pavements with sprayed seals. *Acta Geotechnica,* 19**,** 5481-5502.

Mia, M. N., Henning, T. F., Costello, S. B. & Mckegg, C. 2015. Life cycle cost analysis to identify the need for drainage renewal in maintenance of road asset: Case Studies from a New Zealand road network.

Monaco, S. 2024. SDG 9. Build Resilient Infrastructure, Promote Inclusive and Sustainable Industrialization, and Foster Innovation. *Identity, Territories, and Sustainability: Challenges and Opportunities for Achieving the UN Sustainable Development Goals.* Emerald Publishing Limited.

Pu, J. 2002. *Use of stiffness for evaluating compactness of cohesive geomaterials.* University of Hawaii at Manoa.

Rahman, M. S. & Erlingsson, S. 2016a. Influence of Post Compaction on the Moisture Sensitive Resilient Modulus of Unbound Granular Materials. *Procedia Engineering,* 143**,** 929-936.

Rahman, M. S. & Erlingsson, S. 2016b. Modelling the moisture dependent permanent deformation behavior of unbound granular materials. *Procedia engineering,* 143**,** 921-928.

Sangsefidi, E., Larkin, T. J. & Wilson, D. J. 2021. The effect of weathering on the engineering properties of laboratory compacted unbound granular materials (UGMs). *Construction and Building Materials,* 276**,** 122242.

Sun, J., Oh, E. & Ong, D. E.-L. 2021. Influence of Degree of Saturation (DOS) on Dynamic Behavior of Unbound Granular Materials. *Geosciences,* 11**,** 89.

Takhellambam, B. S., Srivastava, P., Lamba, J., Zhao, W., Kumar, H., Tian, D. & Molinari, R. 2024. Artificial neural network-empowered projected future rainfall intensity-duration-frequency curves under changing climate. *Atmospheric Research,* 297**,** 107122.

Tatsuoka, F. & Correia, A. G. 2018. Importance of controlling the degree of saturation in soil compaction linked to soil structure design. *Transportation Geotechnics,* 17**,** 3-23.

Udukumburage, R. S., Gallage, C. & Dawes, L. 2019. Oedometer based estimation of vertical shrinkage of expansive soil in a large instrumeted soil column. *Heliyon,* 5.

Wang, X., Huang, G. & Liu, J. 2014. Projected increases in intensity and frequency of rainfall extremes through a regional climate modeling approach. *Journal of Geophysical Research: Atmospheres,* 119.

Weerasinghe, I. A., Gallage, C. & Dawes, L. 2019. Optimising geosynthetic clay liner overlaps: implications on hydraulic performance. *Environmental Geotechnics,* 8**,** 264-273.

Xiao, Y., Zheng, K., Chen, L. & Mao, J. 2018. Shakedown analysis of cyclic plastic deformation characteristics of unbound granular materials under moving wheel loads. *Construction and Building Materials,* 167**,** 457-472.